Roles of the Heme Distal Residues of FixL in O_2 Sensing: A Single Convergent Structure of the Heme Moiety Is Relevant to the Downregulation of Kinase Activity†

Atsunari Tanaka,[‡,§] Hiro Nakamura,[‡,§] Yoshitsugu Shiro,*[,§] and Hiroshi Fujii[||]

Yokohama City University International Graduate School of Arts and Sciences, Suehiro, Tsurumi, Yokohama, Kanagawa 230-0045, Japan, RIKEN Harima Institute/SPring-8, Mikazuki, Sayo, Hyogo 679-5148, Japan, and Okazaki Institute for Integrative Bioscience, National Institutes of Natural Sciences, Myodaiji, Okazaki, Aichi 444-8787, Japan

Received September 30, 2005; Revised Manuscript Received December 6, 2005

ABSTRACT: FixL is a heme-based O_2 sensor, in which the autophosphorylation is regulated by the binding of exogenous ligands such as O_2 and CN^-. In this study, mutants of the heme distal Arg200, Arg208, Ile209, Ile210, and Arg214 residues of *Sm*FixL were characterized biochemically and physicochemically, because it has been suggested that they are significant residues in ligand-linked kinase regulation. Measurements of the autoxidation rate, affinities, and kinetics of ligand binding revealed that all of the above residues are involved in stabilization of the O_2−heme complex of FixL. However, Arg214 was found to be the only residue that is directly relevant to the ligand-dependent regulation of kinase activity. Although the wild type and R214K and R214Q mutants exhibited normal kinase regulation, R214A, R214M, R214H, and R214Y did not. ^{13}C and ^{15}N NMR analyses for $^{13}C^{15}N^-$ bound to the truncated heme domains of the Arg214 mutants indicated that, in the wild type and the foregoing two mutants, the heme moiety is present in a single conformation, but in the latter four, the conformations fluctuate possibly because of the lack of an interaction between the iron-bound ligand and residue 214. It is likely that such a rigid conformation of the ligand-bound form is important for the downregulation of histidine kinase activity. Furthermore, a comparison of the NMR data between the wild type and R214K and R214Q mutants suggests that a strong electrostatic interaction between residue 214 and the iron-bound ligand is not necessarily required for the single convergent structure and eventually for the downregulation of FixL.

Nitrogenase catalyzes the reduction of dinitrogen (N_2) into ammonia (NH_3) in rhizobia (*1*, *2*). Because the enzyme is irreversibly inactivated by O_2, a low O_2 tension is necessary for the expression of the enzyme. *Sinorhizobium meliloti* (*Sm*)[1] uses a FixL/FixJ system, which belongs to the ubiquitous two-component signal transduction systems (*3*), as a biological O_2 sensor to control the expression of nitrogenase under microaerobic conditions. FixL consists of a heme-based O_2 sensor domain and an ATP-dependent histidine kinase domain. The kinase activity is enhanced by the dissociation of O_2 from the ferrous iron of the heme at low O_2 concentrations. Activated FixL autophosphorylates a conserved histidine using ATP as the donor, and the phosphoryl group is transferred to a conserved asparate located in a transcription factor, FixJ (*4*−*11*). Phosphorylated FixJ forms a homodimer and binds to promoters of the *nif*A and *fix*K genes to stimulate the expression of nitrogenase (*12*−*21*).

To understand the mechanisms of the ligand-dependent regulation of the kinase activity of FixL, three issues must be evaluated at the molecular level: (i) conformational change of the sensor domain upon the ligand association/dissociation to/from the heme iron, (ii) intramolecular signal transduction from the sensor domain to the catalytic domain, and (iii) activation or inactivation of the catalytic domain. Concerning the first issue, studies of kinase activities of the various liganded FixL complexes indicate that high-spin FixLs have full kinase activities and, in low-spin FixLs, the activity is downregulated, suggesting a correlation between the electronic spin state of the heme iron and the regulation of activity (*22*). Indeed, binding of cyanide (CN^-) to the ferric heme can suppress the kinase activity of FixL, in place of O_2 binding to the ferrous heme (*22*−*25*). However, it was recently reported that CO− and NO−FixLs in the low-spin state have partially downregulated kinase activities; therefore, the correlation between the spin state and kinase activity is either nonexistent or slight (*23*−*25*).

† The work was supported, in part, by the Molecular Ensemble Research in RIKEN and a Grant-in-Aid for Scientific Research of Priority Areas on Metal Sensors (number 12147210) from the Ministry of Education, Culture, Sports, Science, and Technology of Japan.

* To whom correspondence should be addressed. Telephone: +81-791-58-2817. Fax: +81-791-58-2818. E-mail: yshiro@riken.jp.

‡ Yokohama City University International Graduate School of Arts and Sciences.

§ RIKEN Harima Institute/SPring-8.

|| National Institutes of Natural Sciences.

[1] Abbreviations: *Bj*, *Bradyrhizobium japonicum*; DEAE, diethylaminoethyl; DTT, dithiothreitol; SD, standard deviation; SOD, superoxide dismutase; *Sm*, *Sinorhizobium meliloti*; Mb, myoglobin; Hb, hemoglobin; NMR, nuclear magnetic resonance; NTA, nitrilotriacetic acid; WT, wild type.

10.1021/bi051989a CCC: $33.50
Published on Web 02/04/2006

The crystal structures of the heme domain provided some notable findings on the difference between the liganded and unliganded forms: the positions of several amino acids at the heme distal side, including the FG loop, were changed upon the binding of a ligand to the heme iron (*26*−*29*). The conformational differences appear to be caused by the formation of a hydrogen bond between the O_2/CN^- bound to the heme and a distal arginine, Arg220, in *Bradyrhizobium japonicum* (*Bj*)FixL (corresponding to Arg214 in *Sm*FixL) and changes in interactions of the heme 6,7-propionates with Arg206 and His214 in *Bj*FixL (corresponding to Arg200 and Arg208 in *Sm*FixL) (Figure 1). The significance of the distal arginine for O_2 sensing was inferred from mutational analyses. The R220A mutant of *Bj*FixL has an extremely low affinity for O_2, and its kinase activity was not downregulated by CN^- binding (*25*). On the other hand, there is no biochemical data to suggest the importance of Arg206 and His214 of *Bj*FixL on kinase regulation. Although the three residues seem to participate in downregulation, details of the regulatory mechanism are not clear. In addition, the Ile209 and Ile210 mutants in *Sm*FixL were found to lose downregulation in the presence of air. These residues were also proposed to be highly flexible, on the basis of resonance Raman and crystallographic studies. As a result, it has been suggested that the motility of Ile209 and Ile210 in the FG loop is important for O_2 sensing (*30*).

Because many of the previous studies on the vicinity of the heme were performed with a truncated sensor domain, the results cannot be directly correlated to ligand-linked kinase regulation. Therefore, whether these findings are truly significant for the O_2-sensing mechanism or not remains unclear. Therefore, in the present study, the ligand-linked kinase regulation, the ligand-binding affinities, the kinetic parameters of the CN^- binding and the autoxidation rates of Arg200, Arg208, Ile209, Ile210, and Arg214 mutants in *Sm*FixL were studied to verify the roles of these residues and roles of the hydrogen-bond network of the heme distal side in the O_2-sening mechanism. Furthermore, we also characterized the heme and the bound ligand of the CN^- forms of the wild type (WT) and the Arg mutants from ^{13}C and ^{15}N nuclear magnetic resonance (NMR) spectral data for iron-bound $^{13}C^{15}N^-$ and resonance Raman spectra in the presence of $C^{14}N^-$ or $C^{15}N^-$. These results led us to propose a novel ligand-linked regulatory mechanism that is independent of changes in the hydrogen-bond network in the heme distal side.

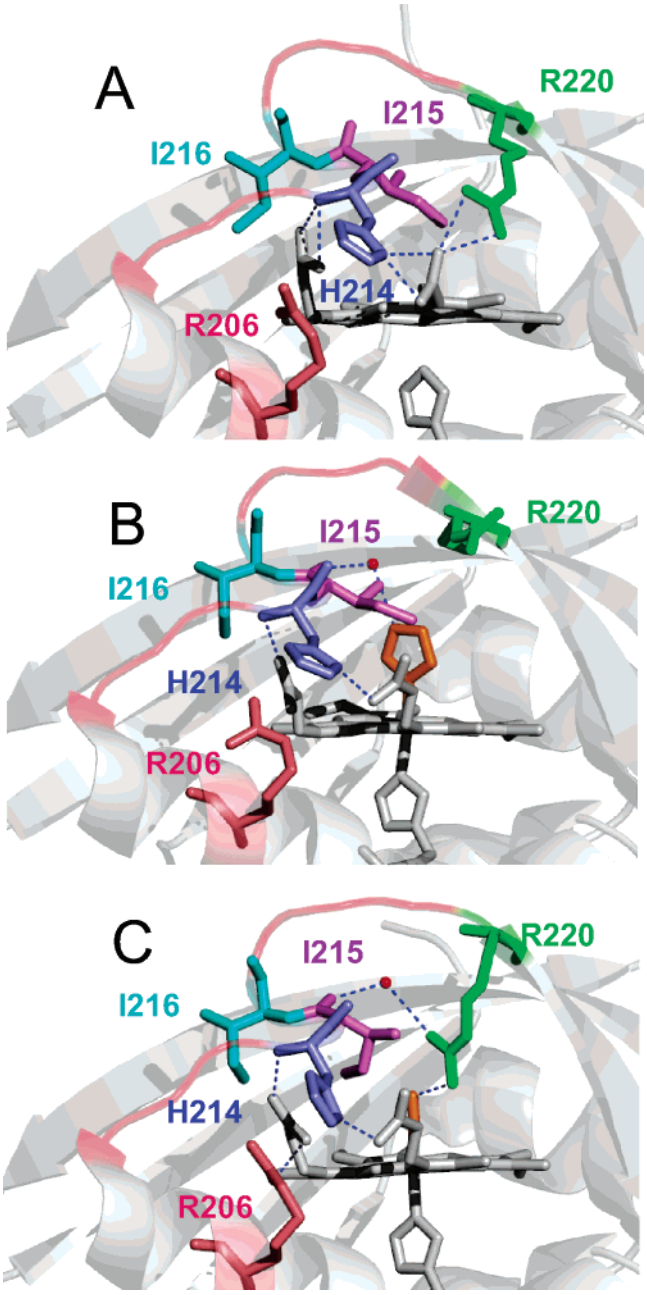

FIGURE 1: Comparison of the tertiary structures of three ferric *Bj*FixLH. (A) met-*Bj*FixLH (PDB ID 1DRM), (B) CN^- met-*Bj*FixLH (PDB ID 1LT0), and (C) imidazole met-*Bj*FixLH (PDB ID 1DP9). The atoms of the heme (white), ligands (orange), proximal histidine (white), and residues (R206, pink; H214, blue violet; I215, violet; I216, cyan; and R220, green), which are thought to play roles in the conformational changes, are depicted as stick models. The red balls represent water molecules. The dash lines show the salt-bridge or hydrogen-bond interactions. The red lines show the FG-loop region. Figures were prepared using PyMOL [DeLano, W. L. (2002) *The PyMOL Molecular Graphics System*, DeLano Scientific, San Carlos, CA].

MATERIALS AND METHODS

Sample Preparation of SmFixL and Its Derivatives. Site-directed mutageneses were carried out by a polymerase chain reaction (PCR) with mutated primers. All constructs were confirmed by DNA sequencing using an ABI310 sequencer (Applied Biosystems). The FixL mutants were produced in *Escherichia coli* strain JM109 with the pUC19-based expression plasmid, pHEL5, which contains an N-terminal 6×His tag and a thrombin cleavage site. The following protein purification procedures were performed on ice or at 4 °C. Cell-free supernatants from JM109 harboring pHEL5-*Sm*fixLJ were produced by two passages through a French press cell (1000 kg/cm^2) and subsequent centrifugation of the homogenates at 75000*g* for 1 h. The supernatants were applied to a Ni−nitrilotriacetic acid (NTA) agarose (QIAGEN) column. The FixL fractions were eluted with a linear gradient of 20−300 mM imidazole in 50 mM potassium phosphate buffer at pH 7.5 containing 150 mM NaCl, 5% glycerol, and 1 mM phenylmethylsulfonyl fluoride. The fractions were applied to a diethylaminoethyl (DEAE)-Sepharose FF (Amasham Bioscience) column and eluted by a linear gradient of 0−500 mM Na_2SO_4 in buffer A (20 mM Tris-H_2SO_4 buffer at pH 8.0 containing 5% glycerol). After

ammonium sulfate was added to the partially purified sample to a final concentration of 1.2 M, precipitates of FixL were obtained by centrifugation at 15000*g* for 10 min and suspended with buffer A containing 700 mM $(NH_4)_2SO_4$. The suspension was applied to a Phenyl-TOYOPEARL 650S (TOSOH) column, and the FixL fractions were eluted using a linear gradient of 700−0 mM $(NH_4)_2SO_4$. After dialysis against buffer A, the purified proteins were concentrated by means of a Centriprep (Amicon) and Centrisart I (Sartorius). The sample was stored at −20 °C in the presence of 40% glycerol.

Sample Preparation of SmFixLH2 and Its Derivatives. Construction of the pHEL5-derived expression plasmids of the truncated heme domain (*Sm*FixLH2), which consists of 129−260 residues of *Sm*FixL, and its Arg214 mutants was carried out by PCR. All constructs were confirmed by DNA sequencing. The FixLH2 proteins were produced in JM109 with the pHEL5 derivatives and purified on a Ni−NTA agarose column, as described above. After dialysis against buffer A, the FixLH2 proteins were digested with thrombin protease (SIGMA) (1 unit/mg of protein) at 25 °C for 5 h to remove the 6×His tag. The samples were applied to a Ni−NTA agarose column, and the cleaved FixLH2 was eluted in the flowthrough fractions using buffer A. The FixLH2 fractions were collected and added with a small amount of APMSF to inactivate thrombin. The purified FixLH2 was concentrated by means of a Centriprep and Centrisart I. Finally, the sample was stored at −20 °C in the presence of 40% glycerol.

Measurement of the Autoxidation Rates of Purified FixLs. FixLs (400 μM) were anaerobically reduced with 2 mM sodium dithionite in 50 μL of a kinase buffer (50 mM Tris-HCl at pH 7.5 and 50 mM KCl) and immediately diluted to a final concentration of 6.7 μM in 3 mL of kinase buffer containing 0.01 unit of superoxide dismutase (SOD) (SIGMA) and 0.01 unit of catalase (SIGMA). The time course for the absorption change at 576 nm was recorded on a SHIMADZU UV-2500PC spectrophotometer with continuous stirring to ensure an adequate supply of air at 37 °C. The autoxidation rate was determined by curve-fitting analysis.

Determination of Ligand-Binding Affinities. All absorption spectra were obtained using a UV-2500PC at 25 °C. Liganded forms of the FixL mutants were prepared by titrating small aliquots of imidazole and KCN solutions into 5 μM met protein in 3 mL of kinase buffer. Visible absorption spectra were recorded when the ligand-binding reached equilibrium. K_d values for imidazole and CN^- were obtained from the absorbance change at 415 and 422 nm, respectively, by curve fitting.

Visible spectra and O_2 equilibrium curves (OECs) were obtained using a UV-2500PC equipped with an oxygenation/deoxygenation cell at 25 °C (*31*). All experiments were performed in the presence of 100 mM dithiothreitol (DTT) to determine $K_d(O_2)$ because the rate of autoxidation of all mutants was too high to maintain the ferrous state in the presence of 10 mM DTT.

Determination of Kinetic Parameters for CN^- Binding to the Distal Arginine Mutants. The generation of the CN^-−FixL complex was monitored at 422 nm by UV-2500PC at 25 °C after mixing the 5 μM met−FixL solution in kinase buffer with small aliquots of the KCN solution at final concentrations of 245, 490, 735, 980, and 1225 μM. CN^-−FixL is assumed to be generated by a pseudo-first-order reaction ($\nu = k_{obs}$[FixL], $k_{obs} = k_{on}[CN^-] + k_{off}$) when [FixL] is much less than $[CN^-]$. Because the actual time course for the change in absorbance at 422 nm for the WT[2] and Arg214 mutants, except the R214H mutant, exhibited monophasic kinetics, the observed rate constant (k_{obs}) was obtained by fitting to an exponential function of $\Delta A_{total} = \Delta A \exp(-k_{obs}t)$. Because the R214H mutant showed biphasic kinetics, the observed rate constants were calculated by fitting to a two-term exponential function of $\Delta A_{total} = \Delta A_{fast} \exp(-k_{obs,fast}t) + \Delta A_{slow} \exp(-k_{obs,slow}t)$. The plots of k_{obs} versus [KCN] exhibited a linear relationship (data not shown), giving the k_{on} values for each phase from the equation $k_{obs} = k_{on}[CN^-] + k_{off}$. The k_{off} values were obtained by multiplying K_d by k_{on}.

Autophosphorylation Assay. The liganded *Sm*FixL mutants were prepared in the presence of 20 mM imidazole and 5 mM KCN, respectively. The procedures used for the measurement of the kinase activity have been described previously (*24*, *32*). When the ligand-binding affinities of the mutants are different from each other, these mutants do not give the same content of the ligand-bound form in the presence of a certain ligand concentration. Thus, we estimated the activities of the fully ligand-bound forms because the kinase activity of FixL is repressed in direct proportion to the ratio of liganded FixL (*22*). The k_{obs}, which is the initial rate of the autophosphorylation activity for the total protein, is given as follows: $k_{obs}[L_{total}] = k_{free}[L_{free}] + k_{bound}[L_{bound}]$, where k_{free} and k_{bound} are the initial rates of the activity for the ligand-free and ligand-bound forms, respectively, and $[L_{total}]$, $[L_{free}]$, and $[L_{bound}]$ are the protein concentration of the total FixL and the ligand-free and ligand-bound forms, respectively. This equation can be rearranged to $k_{bound} = (k_{obs}[L_{total}] - k_{free}[L_{free}])/[L_{bound}]$. I_{ph}, obtained by dividing the k_{free} by the k_{bound}, was defined as the inhibition factor for autophosphorylation.

^1H, ^{13}C, and ^{15}N NMR Spectral Measurements. The NMR measurements require a high concentration of hemoproteins (∼4 mM) to obtain satisfactory signals, because the ^{13}C and ^{15}N signals derived from the heme iron-bound $^{13}C^{15}N^-$ are very weak. However, solutions of full-length FixL can be prepared at concentrations up to about 1.5 mM. Therefore, we prepared the truncated heme domain named FixLH2, which can be highly concentrated and stable, for the NMR measurements. The samples were prepared as follows. The $^{13}C^{15}N^-$−FixLH2 mutant (∼3−4 mM) was dissolved in D_2O buffered with 0.1 M potassium phosphate at pH 7.0 in the presence of excess $K^{13}C^{15}N$. ^1H, ^{13}C, and ^{15}N NMR spectra of $^{13}C^{15}N^-$−FixLH2 were taken on a JEOL Lambda-500 spectrometer. ^1H NMR spectra were obtained in sweep widths of 50 kHz using 32 K data points. ^{13}C NMR spectra were typically obtained in sweep widths of 200 kHz at 125.27 MHz using 4 K data points. ^{15}N NMR spectra were obtained in sweep widths of 100 kHz at 50.73 MHz using 4 K data points. The pulse repetition time and pulse width were 0.075 s and 8 ms, respectively. Typically 1 000 000 transients were

[2] All of the variants, except for the FixLH2 mutants, were constructed in the C301A background to measure kinase activities in the stable ferric state because the inactivation of the wild-type kinase is caused by aberrant disulfide bond formation at Cys301 in the ferric homodimer (*24*). In this paper, the C301A FixL is referred to as the WT.

Table 1: Comparison of Autoxidation Rates of the *Sm*FixL Mutants

*Sm*FixL mutants	(h^{-1})	*Sm*FixL mutants	(h^{-1})
WT	0.99	R214M	14
R200A	3.7	R214H	51
R208A	11	R214Q	19
I209A	5.6	R214K	19
I210A	16	R214Y	19
R214A	14		

collected for FixLH2. Chemical shift values of the ^{13}C and ^{15}N NMR spectra are referenced to external tetramethylsilane (TMS) in chloroform and sodium nitrate ($^{15}NO_3^-$) in deuterium oxide, respectively.

Resonance Raman Measurements. The CN^--bound forms of the WT and R214K and R214Q mutants were dissolved in the kinase buffer containing 500 μM KCN or K^{15}N in the kinase buffer. The CN^-−R214M and −R214A mutants were prepared in the presence of 5 mM KCN or K^{15}N. Resonance Raman spectra of the cyanide adducts were obtained using a JASCO NR-1800 spectrometer, equipped with a liquid nitrogen-cooled CCD detector (Princeton Instruments) and operated in the single-dispersion mode. The slit width for the spectral measurements was 4 cm^{-1}. An excitation light at 413.1 nm was generated using a Kr^+ laser (Coherent, Innova 90). The laser power was maintained at less than 5 mW at the sample point. Holographic filters (Kaiser Optical Systems, Inc.) were used to eliminate the Rayleigh scattering. The cylindrical Raman cell containing about 25 μM sample solution was kept spinning to minimize local heating. The Raman spectrometer was calibrated for each measurement using indene (Wako Chemicals) as the standard. Optical absorption spectra of the cyanide adducts were measured with a spectrometer (SHIMADZU UV-2500-PC) before and after the resonance Raman measurements.

RESULTS

Effect of Mutations on the Autoxidation Rate. The autoxidation rates of the WT and I209A and I210A mutants were consistent with previously described data (*33*, *34*). The R200A and I209A mutants exhibited autoxidation rates that were approximately 3- and 5-fold faster than the WT (Table 1). The R208A, R210A, R214A, R214M, R214Q, R214K, and R214Y mutants showed 10−20 times faster autoxidation rates (∼11−19 h^{-1}). The autoxidation rate of the R214H mutant was about 50 times as fast as the WT (Table 1). Notably, the R214H mutant exhibited an optical absorption spectrum in the ferric state, which is entirely different from those of the WT and the other mutants. While the Soret bands of the WT and the other mutants were observed at ∼395−398 nm, the Soret band of the R214H mutant was located at 406 nm, similar to the case for WT myoglobin (Mb) and its H64V/V68H double mutant (*35*). The spectral characteristics suggest that a water molecule is present at the heme sixth coordination site of the ferric R214H analogous to Mb. This suggests that the heme pocket of the FixL mutants, especially of the R214H mutant, is easily accessible to water molecules. Therefore, the extremely enhanced rate of autoxidation of the R214H mutant could be explained in terms of a nucleophilic attack by a water molecule on the Fe−O_2 moiety, and this explanation might be extrapolated to other mutants of FixL.

Table 2: O_2, Imidazole, and CN^- Binding Affinities for the Mutants

	K_d (μM)		
*Sm*FixL mutants	O_2[a]	imidazole	CN^-
WT	33 ± 3	2200	12
R200A	79 ± 9	1200	19
R208A	120 ± 10	420	9.4
I209A	42 ± 2	270	4.1
I210A	ND[b]	930	10
R214A	ND	1300	960
R214M	ND	850	550
R214H	54 ± 4	690	6
R214Q	64 ± 6	1200	36
R214K	ND	1100	44
R214Y	ND	1300	440

[a] Values for O_2 are given as the mean ± SD. [b] ND = not determined.

O_2, Imidazole, and CN^- Binding Affinities of the SmFixL Mutants. As were compiled and compared in Table 2, the ligand-binding affinities, especially for O_2, of FixL were sensitive and vulnerable to a mutation in the distal residues. The $K_d(O_2)$ of the I209A mutant in the ferrous state was nearly equal to that of the WT, but the R200A, R208A, R214H, and R214Q mutants showed lower affinities than the WT by ∼1.6−3.6 times. Because the affinities of the R210A, R214A, R214M, R214K, and R214Y mutants were very low, their K_d values could not be determined. Indeed, absorption spectral profiles of these mutants at 250−300 μM O_2 exhibited the deoxy form (data not shown). Because the met and deoxy forms have high kinase activities, it is difficult to evaluate the mutational effects on the kinase activity of the O_2-bound mutants that undergo very rapid autoxidation and have a low O_2 affinity. Thus, we characterized the CN^-- and imidazole-bound forms of the mutants, because CN^- and imidazole binding to the ferric FixL represses the kinase activity of the met form, similar to O_2 binding to the ferrous FixL (*24*, *33*).

The K_d values (CN^-) of the R200A, R208A, I209A, and I210A mutants were similar to that of the WT. In contrast, remarkable changes were observed in the case of the Arg214 mutants. The R214A, R214M, and R214Y mutants showed a dramatically low affinity. However, the affinity of the R214Q and R214K mutants was ∼3−4 times lower than that of the WT, and the affinity of the R214H mutant was nearly identical to that of the WT.

All of the mutants had higher imidazole-binding affinities than the WT in the ferric state. In particular, the Ile208, Ile209, and some of the Arg214 mutants showed higher imidazole-binding affinities. As the steric hindrance of the residues at the 208, 209, and 214 positions (Figure 1) in the mutants is diminished, thus widening the heme pocket, the bulky ligand (imidazole) might easily enter the iron coordination sphere. This might explain why the imidazole-binding affinity of the mutants is higher than that of the WT.

Kinetic Parameters for CN^- Binding of the Distal Arginine Mutants. Because some of the Arg214 mutants showed low CN^--binding affinities, the kinetic parameters for CN^- binding of the mutants were studied (see Table 3). For the R214A, R214M, and R214Y mutants, which show substantially low CN^--binding affinities, the k_{on} and k_{off} values were approximately 10-fold lower and 10-fold higher, respectively, than those of the WT. The k_{on} values for the R214K and

Table 3: Kinetic Parameters for CN^- Binding to the Distal Arginine Mutants

FixL	k_{on} (μM^{-1} s^{-1}) fast phase	k_{on} (μM^{-1} s^{-1}) slow phase	k_{off} (s^{-1})
WT	2.6×10^{-5}		3.1×10^{-4}
R214A	3.2×10^{-6}		3.1×10^{-3}
R214M	3.0×10^{-6}		1.7×10^{-3}
R214H	1.1×10^{-5}	7.3×10^{-5}	
R214Q	1.2×10^{-5}		4.3×10^{-4}
R214K	4.8×10^{-5}		2.1×10^{-3}
R214Y	5.3×10^{-6}		2.3×10^{-3}

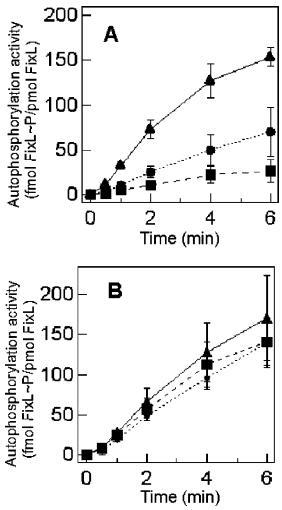

FIGURE 2: Autophosphorylation activities of the ferric *Sm*FixL (A) WT and (B) R214M mutants. (▲) met, (●) imidazole, and (■) CN^- complex. Values are given as the mean ± standard deviation (SD).

R214Q mutants are similar to that of the WT, whereas the k_{off} value of the R214K mutant is 7-fold higher than the value of the WT.

Regulation of Ligand-Linked Autophosphorylation in the Ferric State. Autophosphorylation of all of the mutants was measured in the ferric form in the presence and absence of CN^- and imidazole, because their oxy forms are too unstable to permit their autophosphorylation activities to be measured. The ligand-dependent regulation of the activities was estimated by inhibition factors (I_{ph}), which can be defined as the ratio of kinase activities of the ligand-bound to the ligand-unbound forms. In the case of the WT (normal regulation), the I_{ph} values were 3.8 (imidazole-linked regulation) and 6.5 (Figure 2A, CN^--linked regulation). It is interesting to note that the autophosphorylation of the R200A, R208A, I209A, and I210A mutants was normally regulated by imidazole and CN^- binding (Table 4). In other words, these residues (Arg200, Arg208, Ile209, and Ile210) are not directly involved in the regulatory mechanism of the kinase reaction.

On the other hand, some of the Arg214 mutants are deficient in terms of repressing autophosphorylation by ligand binding. The imidazole-dependent regulation of the R214M, R214H, R214Q, and R214Y mutants was abolished (Figure 2B, I_{ph} = ~1.1−1.5), while the activity of the imidazole-bound R214A and R214K mutants was as low as that of the WT (Table 4). Regulation by CN^- was very loose in the R214A, R214M, and R214H mutants (Figure 2B, I_{ph} = 1.6, 1.2, and 2.0). Meanwhile, the R214Q and R214K mutants showed regulation similar to the WT (Table 4). The

Table 4: Inhibition of the Initial Rate of the Autophosphorylation (k_{ph}) of *Sm*FixL Mutants by Ligand Binding

FixL	autophosphorylation k_{ph}[a] (autophosphorylation[b]/min) met	imidazole	CN^-	inhibition factor I_{ph}[c] imidazole	CN^-
WT	33	8.6	5.1	3.8	6.5
R200A	83	24	4.2	3.5	20
R208A	53	11	8.7	4.8	6.1
I209A	45	17	8.5	2.6	5.3
I210A	138	15	13	9.2	11
R214A	28	7.5	17	3.7	1.6
R214M	28	19	24	1.5	1.2
R214H	22	17	11	1.3	2.0
R214Q	17	13	4.3	1.3	4.0
R214K	26	9.1	5.9	2.9	4.4
R214Y	16	14	45	1.1	0.36

[a] k_{ph} of met forms are actual values, and k_{ph} of imidazole- and CN^--bound forms are calculated values (see the Materials and Methods). [b] fmol of FixL~P/pmol of FixL. [c] $I_{ph} = k_{free}/k_{bound}$.

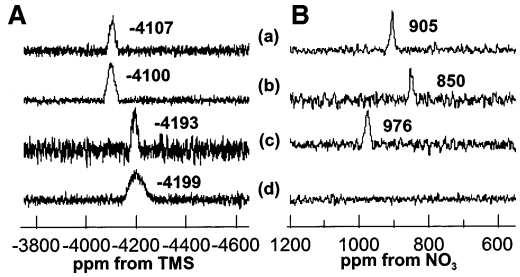

FIGURE 3: NMR spectra of iron-bound $^{13}C^{15}N$ of the CN^- complexes of ferric *Sm*FixLH2s. A and B show the ^{13}C and ^{15}N NMR spectra, respectively. (a) WT and (b) R214K, (c) R214Q, and (d) R214H mutants.

autophosphorylation activity of the R214Y−CN^- complex was higher than that of the met form (Table 4).

^{13}C and ^{15}N NMR Spectra of the $^{13}C^{15}N^-$ Forms of SmFixLH2 and Its Derivatives. In this study, we found that only the Arg214 residue is directly involved in the ligand-linked kinase regulation mechanism of FixL. To examine how the Arg214 residue functions in the regulation, ^{13}C and ^{15}N NMR spectra were obtained for the WT and the Arg214 mutants in their $^{13}C^{15}N^-$ forms. It has been known that ^{13}C NMR spectroscopy of the $^{13}C^{15}N^-$ forms is a good tool for characterizing the property of the proximal ligand, while ^{15}N NMR spectra are sensitive to structural characteristics both in the heme distal and proximal side (*36*−*42*).

The ^{13}C and ^{15}N NMR signals of the iron-bound $^{13}C^{15}N^-$ for the WT FixLH2 were located at −4107 and 905 ppm, respectively (Figure 3a). These NMR shifts are possibly derived from the neutral imidazole as a fifth ligand and the hydrogen-bonding interaction of the Arg214 side chain with the iron-bound $^{13}C^{15}N^-$, respectively (*36*). The ^{13}C NMR signals of R214K and R214Q were located at −4100 and −4193 ppm, respectively. For a comparison, it is noteworthy that the signals of $^{13}CN^-$ complexes of heme peroxidases, which have an anionic imidazole (imidazolate) as a fifth ligand, are at −3543 ppm, while those of Mb and hemoglobin (Hb), with a neutral imidazole ligand, are at −4145 and −4074 ppm, respectively (*36*). Therefore, the difference in the position of the ^{13}C NMR signal between the WT and R214K and R214Q mutants (~90 ppm) was relatively small, indicating that the structure at the heme fifth side was not significantly altered upon the Arg214 mutation to Lys or Gln.

Table 5: Comparison of ^{13}C and ^{15}N NMR Shifts of Iron-Bound $^{13}C^{15}N$ of CN^- Complexes of *Sm*FixL

*Sm*FixL mutant	^{13}C NMR signal (ppm)	^{15}N NMR signal (ppm)
*Sm*FiLH	−4107	905
R214A *Sm*FixLH2	ND[a]	ND
R214M *Sm*FixLH2	ND	ND
R214H *Sm*FixLH2	−4199	ND
R214K *Sm*FixLH2	−4100	850
R214Q *Sm*FixLH2	−4193	976
R214Y *Sm*FixLH2	ND	ND

[a] ND = not detected.

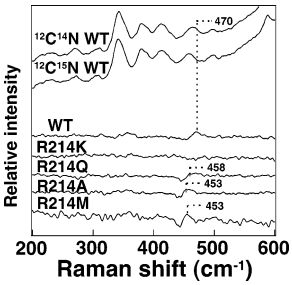

FIGURE 4: Resonance Raman spectra (low-frequency regions) of *Sm*FixL and its 214 mutants in the CN^- form. Upper two spectra indicate the resonance Raman spectra of the WT in the $^{12}C^{14}N^-$ and $^{12}C^{15}N^-$ forms. Lower five spectra show the difference spectra ($^{12}C^{14}N^-$ − $^{12}C^{15}N^-$ form) of the WT and Arg214 mutants.

On the other hand, the ^{15}N NMR signal is located at 850 ppm for R214K, while it is at 976 ppm for R214Q. These upfield (∼70 ppm) and downfield (∼50 ppm) shifts upon the Lys214 and Gln214 mutation, respectively, appear to be significant. The results are comparable to those in an ^{15}N NMR study of the $C^{15}N^-$ complex of cytochrome P450cam; i.e., the difference of the ^{15}N NMR shifts (d-camphor-bound − d-camphor-free) was 67 ppm (*39*). The difference in ^{15}N NMR signal is thought to reflect the presence or absence of an interaction of the iron-bound $C^{15}N^-$ with d-camphor, the bound substrate. It is, thus, likely that the interaction of the iron-bound CN^- with the 214 residue (Lys or Gln) in the Arg214 mutants is different from that in the WT and that the 214 mutation effect is opposite between Lys and Gln. While the ^{13}C NMR signal for the R214H mutant was located at −4199 ppm but was very broad, the ^{15}N NMR signal could not be detected. Furthermore, in the other Arg214 mutants (R214A, R214M, and R214Y), the ^{13}C and ^{15}N NMR signals were not detected (Table 5).

Resonance Raman Spectra of CN$^-$*−FixLs*. To gain further insight into the interaction of the iron-bound CN^- with the 214 residue, the resonance Raman spectra of the WT *Sm*FixL and its Arg214 mutants (R214A, R214K, R214M, and R214Q) in the presence of $C^{14}N^-$ or $C^{15}N^-$ were measured. Despite a low signal-to-noise ratio, a CN-sensitive band was observed at 470 cm^{-1} for the WT and attributed to the Fe−CN stretching mode, ν_{Fe-CN}. Although the spectrum was not well-resolved for the R214K mutant, the ν_{Fe-CN} bands were observed at 458, 453, and 453 cm^{-1} in the R214Q, R214M, and R214A mutants, respectively (Figure 4). The low-frequency shifts upon the mutation seem to be similar to the observation in the Fe−O_2 stretching mode for the truncated heme domain of *Bj*FixL, WT (573 cm^{-1}) and R220Q mutant (563 cm^{-1}) (*43*). According to the ν_{Fe-CN} data for the Mb mutants (*44*), the observed shifts of ν_{Fe-CN} in the FixL mutants suggest that the Fe−C−N coordination geometry may be more linear than that of the WT. Because the mutants with a different size of the side chain show similar linear coordination, the heme-bound CN^- may not interact with the mutated residues at 214.

These results, in combination with the NMR results, will be discussed further in relation to protein fluctuation, the ligand interaction, and kinase regulation in the Discussion.

DISCUSSION

Conformational changes around the heme of FixL induced by the binding of various ligands have been extensively studied at the atomic level, but the relation between the structural changes and kinase regulation has not been disclosed. We systematically characterized mutations in the heme pocket residues, which are suggested to play roles in kinase regulation.

Significance of Interactions among the Arg200 and Arg208 Residues and the Heme Propionates. Salt bridges among the Arg206, His214 residues, and heme propionates were present in the crystal structures of *Bj*FixLH, and the interactions are altered between the unliganded (kinase activity "on") and liganded (kinase activity "off") forms (*26*, *28*, *29*). Such an interaction also seems to be present between the Arg200, Arg208, and heme propionates in the met form of *Sm*FixLH (*27*). Thus, the changes appear to be a key factor in the kinase regulation mechanism. However, in the case of the R200A and R208A mutants, the regulation of autophosphorylation by imidazole and CN^- binding was normal despite the absence of such interactions. Furthermore, these mutants showed O_2-linked regulation in air-saturated buffer (data not shown). It should be noted that their O_2-linked regulations were slightly looser than that of the WT, because the amount of the oxy form of the mutants probably decreased because of the rapid autoxidation rates and low O_2-binding affinities. These results clearly indicate that the ligand-linked regulation of autophosphorylation does not require salt-bridge interactions among Arg200, Arg208, and the heme propionates.

The rapid rate of autoxidation and the low O_2-binding affinities of the Arg200 and Arg208 mutants may be caused by the absence of an interaction among these two residues and the heme propionates. For example, upon the K45S mutation of Mb, the heme 6-propionate lost any interactions and the solvent-exposed side of the heme pocket was opened more widely, allowing an increase in the accessibility of solvent nucleophiles (*45*). The structural change as the result of the mutation caused a 7-fold increase in the autoxidation rate of Mb (*46*). By analogy, electrostatic interactions among Arg200, Arg208, and the heme propionates in *Sm*FixL would function to stabilize a closed conformation, preventing the entrance of nucleophiles (water molecules) into the heme pocket.

Roles of the Ile209 and Ile210. The I209A and I210A mutants also showed normal kinase regulation as a result of imidazole and CN^- binding. These results are inconsistent with previous data, indicating that kinase reactions of these mutants cannot be regulated by O_2 binding (*30*). However, because of the rapid autoxidation rates and low O_2-binding affinities, the Ile209 and Ile210 mutants in the presence of 10 mM DTT or 50 mM β-mercaptoethanol in air-saturated buffer are comprised of a mixture of three forms: the kinase inactive oxy form, the active deoxy form, and the active met

form. Hence, these variants appear to be deficient not in O_2-linked kinase regulation but in the stability of the oxy form.

Previous resonance Raman studies have suggested that the strength of the hydrogen bond of the heme propionates in these mutants is weaker than that in the WT, and steric hindrance between the O_2 bound to the heme and the residues are also diminished (*30*). The high affinities found for the mutants for a bulky ligand (imidazole) might also be induced by this diminution. Accordingly, the instability of the oxy form of the mutants can be explained by an increase in the accessibility of nucleophiles because of the expansion of the distal heme pocket induced by the rearrangement of the interactions.

Role of the Distal Arg214. In the crystal structure of the kinase-activated met form of WT FixLH (*26*), the Arg214 residue binds to the heme 7-propionate through electrostatic interactions. In the Arg214 mutants, such as R214A, where the interaction appears to be lost, maximal kinase activity retained for the met form regardless of the length, size, and polarity of the side chain, suggesting that the Arg214−7-propionate interaction is not important for kinase activation. On the other hand, the Arg214 mutation significantly affected the imidazole- and CN^--linked downregulation of the kinase activity of FixL. Indeed, the CN^- forms of the R214A and R214M mutants lost regulation (I_{ph} = 1.6 and 1.2), whereas those of the R214K and R214Q mutants exhibited normal kinase regulation (I_{ph} = 4.4 and 4.0). Thus, the residue at the 214 position appears to be significant for kinase inactivation.

The resonance Raman data suggest that an interaction between the heme-bound CN^- and the 214 residue observed in the WT is lost in the R214Q, R214M, and R214A mutants because of these mutational effects. The R214Q mutant downregulates the kinase activity in the CN^- form, but the CN^- forms of the R214M and R214A mutants constitutively have high activities such as the met form, as described above. Therefore, the interaction may not be necessarily for the kinase regulation.

To understand why the R214M and R214A mutants show the constitutive activity, roles of the 214 residue are next discussed on the basis of chemical information of the ligand and heme moiety in the WT and the 214 mutants obtained by detailed NMR analysis. The NMR measurements provided an interesting correlation between detection of NMR signals and the kinase repression. For the R214K and R214Q mutants as well as the WT, the ^{13}C and ^{15}N NMR signals of the iron-bound ligand are detectable (the NMR-detectable mutants), while those of the R214A and R214M mutants are not detectable (the NMR-undetectable mutants). The absence of NMR signals seems to depend upon instability associated with the CN^- binding to the ferric iron, because the NMR-undetectable mutants exhibited an extremely low affinity for CN^-. However, the dissociation rate constants for CN^- in these mutants were not always larger than those of the NMR-detectable mutants and the WT: e.g., the k_{off} value for the R214M mutant (0.0017 s^{-1}) is similar to that of the R214K mutant (0.0021 s^{-1}). Rather, the association rate constants for CN^- in the undetected mutants ($\sim 10^{-6}$ μM^{-1} s^{-1}) are smaller than those of the detectable mutants and the WT ($\sim 10^{-5}$ μM^{-1} s^{-1}), suggesting that protein dynamics could be related to whether the NMR signals are detected or not. Indeed, corresponding to the ^{13}C and ^{15}N NMR observations for the Arg214 mutants, the heme methyl ^1H NMR signals of the NMR-undetectable mutants were very broad (data not shown) (*47*). Because the global fold of the Arg214 mutant would be expected to be similar to that of the WT (*25*), this suggests that the conformations of these mutant proteins in the heme vicinity of the CN^--bound form fluctuate or are destabilized. The conformation around the heme in the NMR-undetectable mutants does not converge into a single form, eventually resulting in the broadening out of the ^{13}C and ^{15}N NMR signals.

The fluctuating conformation in the R214A and R214M mutants could be undesirable for the downregulation of kinase activity. In the case of the R214H mutant, the ^{15}N NMR signal was not detected but the broad ^{13}C NMR signal was detected, possibly because the sensitivity of the ^{13}C NMR signal is generally better than that of the ^{15}N NMR signal. Therefore, it seems reasonable to conclude that the conformation of the R214H mutant would partly fluctuate but that the rigid fraction might also be present in the solution unlike the other NMR-undetectable mutants. The mixture of the fluctuated and rigid fractions might cause the biphasic action for CN^- binding. This suggestion is consistent with the CN^--linked kinase regulation in the R214H mutant (I_{ph} = 2.0), which is stronger than those of the R214M and the R214A mutants (I_{ph} = 1.6 and 1.2) but weaker than those of the WT and R214K and R214Q mutants (I_{ph} = 6.5, 4.4, and 4.0).

The fluctuating or destabilized conformation in the CN^--bound forms of the R214A and R214M mutants could be caused by the absence of an interaction of the 214 residue with the iron-bound ligand (CN^-). In the case of the WT, the Arg214 side chain interacts with the iron-bound CN^- through electrostatic or hydrogen-bonding interactions, as evidenced in the X-ray crystal structure (*29*), indicating a single conformation and eventually normal kinase regulation. Such rigid and converged structural characteristics in the heme environment were thought to provide the well-resolved ^{13}C and ^{15}N NMR signals of the iron-bound $^{13}C^{15}N^-$ at −4107 and 905 ppm, respectively.

The R214K and R214Q mutants also exhibited normal kinase regulation, and consistently well-resolved ^{13}C and ^{15}N NMR signals were observed, indicating a single (nonfluctuating) conformation. The positions of the ^{13}C and ^{15}N NMR signals in the case of the Arg214 mutants suggest that the proximal structure was not altered (*36*), while the distal structure, especially the interaction of the iron-bound CN^- with the 214 residue, was affected. The fact that the side chain of Lys is positively charged suggests that Lys214 could interact with the iron-bound CN^- to the same extent as or stronger than Arg214. On the other hand, the interaction of the CN^- ligand with the neutral amide of Gln214 in the R214Q mutant might be weak or missing, which is consistent with the data of resonance Raman spectra. Because the R214Q mutant showed an enhanced autoxidation rate, a water molecule appears to be present in close proximity to the iron-bound O_2. If such a structure is possibly the case for the CN^--bound form, the water molecule may intervene to generate a weak interaction. On the basis of these observations, we conclude that the single (nonfluctuating) conformation is significant for the downregulation of the kinase activity, but a strong interaction between the 214

residue and the iron-bound ligand may not be necessarily required.

Despite the large volume of structural information for Arg200, Arg208, Ile209, and Ile210 on the salt bridge and the hydrogen-bond network, the present mutational studies show that they are not directly involved in the downregulation of kinase activity but contribute to the formation of a stable O_2−heme complex. Concerning the function of FixL as the O_2 sensor *in vivo*, it is important to form a stable O_2−heme complex at high O_2 tensions. Therefore, the autoxidation reaction should be repressed as much as possible. In contrast, Arg214 is shown to play roles in the direct trigger, not only the stabilizer of the O_2 form. Although we cannot completely ensure that the conclusion elicited from the data of the CN^- complex explains the O_2-linked kinase regulation, the concept that a single convergent structure is responsible for the downregulation of kinase activity is unique and will cast a new light on the mechanism of regulation of the two-component systems.

ACKNOWLEDGMENT

We thank Ms. Hitomi Sawai (Himeji Institute of Technology/University of Hyogo) for technical assistance of the resonance Raman measurements and useful discussions.

REFERENCES

1. Hill, S. (1988) How is nitrogenase regulated by oxygen, *FEMS Microbiol. Rev. 54*, 111−129.
2. Hunt, S., and Layzell, D. B. (1993) Gas exchang of legume nodules and the regulation of nitrogenase activity, *Annu. Rev. Plant Physiol. Plant Mol. Biol. 44*, 483−511.
3. Stock, A. M., Robinson, V. L., and Goudreau, P. N. (2000) Two-component signal transduction, *Annu. Rev. Biochem. 69*, 183−215.
4. David, M., Daveran, M. L., Batut, J., Dedieu, A., Domergue, O., Ghai, J., Hertig, C., Boistard, P., and Kahn, D. (1988) Cascade regulation of *nif* gene expression in *Rhizobium meliloti*, *Cell 54*, 671−683.
5. de Philip, P., Batut, J., and Boistard, P. (1990) *Rhizobium meliloti* FixL is an oxygen sensor and regulates *R. meliloti nifA* and *fixK* genes differently in *Escherichia coli*, *J. Bacteriol. 172*, 4255−4262.
6. Gilles-Gonzalez, M. A., Ditta, G. S., and Helinski, D. R. (1991) A heamoprotein with kinase activity encoded by the oxygen sensor of *Rhizobium meliloti*, *Nature 350*, 170−172.
7. Monson, E. K., Weinstein, M., Ditta, G. S., and Helinski, D. R. (1992) The FixL protein of *Rhizobium meliloti* can be separated into a heme-binding oxygen sensing domain and a functional C-terminal kinase domain, *Proc. Natl. Acad. Sci. U.S.A. 89*, 4280−4284.
8. de Philip, P., Soupene, E., Batut, J., and Boistard, P. (1992) Modular structure of the FixL protein of *Rhizobium meliloti*, *Mol. Gen. Genet. 235*, 49−54.
9. Lois, A. F., Weinstein, M., Ditta, G. S., and Helinski, D. R. (1993) Autophosphorylation and phosphatase activities of the oxygen-sensing protein FixL of *Rhizobium meliloti* are coordinately regulated by oxygen, *J. Biol. Chem. 268*, 4370−4375.
10. Gilles-Gonzalez, M. A., and Gonzalez, G. (1993) Regulation of the kinase activity of heme protein FixL from the two-component system FixL/FixJ of *Rhizobium meliloti*, *J. Biol. Chem. 268*, 16293−16297.
11. Monson, E. K., Ditta, G. S., and Helinski, D. R. (1995) The oxygen sensor protein, FixL, of *Rhizobium meliloti*, *J. Biol. Chem. 270*, 5243−5250.
12. Batut, J., Santero, E., and Kustu, S. (1991) *In vitro* activity of the nitrogen fixation regulatory protein FixLJ from *Rhizobium meliloti*, *J. Bacteriol. 173*, 5914−5917.
13. Agron, P. G., Ditta, G. S., and Helinski, D. R. (1992) Mutational analysis of the *Rhizobium meliloti* nifA promoter, *J. Bacteriol. 174*, 4120−4129.
14. Anthamatten, D., Scherb, B., and Hennecke, H. (1992) Characterization of a *fixLJ*-regulated *Bradyrhizobium japonicum* gene sharing similarity with the *Echerichia coli fnr* and *Rhizobium meliloti fix*K genes, *J. Bacteriol. 174*, 2111−2120.
15. Galinier, A., Garnerone, A. M., Reyrat, J. M., Kahn, D., Batut, J., and Boistard, P. (1994) Phosphorylation of the *Rhizobium meliloti* FixJ protein induces its binding to a compound regulatory region at the *fixK* promorter, *J. Biol. Chem. 269*, 23784−23789.
16. Reyrat, J. M., David, M., Batut, J., and Boistard, P. (1994) FixL of *Rhizobium meliloti* enhances the transcriptional activity of a mutant FixJD45N protein by phosphorylation of an alternate residue, *J. Bacteriol. 176*, 1969−1976.
17. Nellen-Anthamatten, D., Rossi, P., Preisig, O., Kullik, I., Babst, M., Fischer, H. M., and Hennecke, H. (1998) *Bradyrhizobium japonicum* $FixK_2$, a crucial distributor in the FixLJ-dependent regulatory cascade for control of genes inducible by low oxygen levels, *J. Bacteriol. 180*, 5251−5255.
18. Da Re, S., Schumacher, J., Rousseau, P., Fourment, J., Ebel, C., and Kahn, D. (1999) Phosphorylation-induced dimerization of the FixJ receiver domain, *Mol. Microbiol. 34*, 504−511.
19. Ton-Hoang, B., Salhi, M., Schumacher, J., Da Re, S., and Kahn, D. (2001) Promoetr-specific involvement of the FixJ receiver domain in transcriptional activation, *J. Mol. Biol. 312*, 583−589.
20. Ferrieres, L., and Kahn, D. (2002) Two distinct classes of FixJ binding sites defined by *in vitro* selection, *FEBS Lett. 517*, 185−189.
21. Ferrieres, L., Francez-Charlot, A., Gouzy, J., Rouille, S., and Kahn, D. (2004) FixJ-regulated genes evolved through promoter duplication in *Sinorhizobium meliloti*, *Microbiology 150*, 2335−2345.
22. Gilles-Gonzalez, M. A., Gonzalez, G., and Perutz, M. F. (1995) Kinase activity of oxygen sensor FixL depends on the spin state of its heme iron, *Biochemistry 34*, 232−236.
23. Tuckerman, J. R., Gonzalez, G., Dioum, E. M., and Gilles-Gonzalez, M. A. (2002) Ligand and oxidation-state specific regulation of the heme-based oxygen sensor FixL from *Sinorhizobium meliloti*, *Biochemistry 41*, 6170−6177.
24. Akimoto S, Tanaka A, Nakamura K, Shiro Y, and Nakamura H. (2003) O_2-Specific regulation of the ferrous heme-based sensor kinase FixL from *Sinorhizobium meliloti* and its aberrant inactivation in the ferric form, *Biochem. Biophys. Res. Commun. 304*, 136−142.
25. Dunham, C. M., Dioum, E. M., Tuckerman, J. R., Gonzalez, G., Scott, W. G., and Gilles-Gonzalez, M. A. (2003) A distal arginine in oxygen-sensing heme−PAS domains is essential to ligand binding, signal transduction, and structure, *Biochemistry 42*, 7701−7708.
26. Gong, W., Hao, B., Mansy, S. S., Gonzalez, G., Gilles-Gonzalez, M. A., and Chan, M. K. (1998) Structure of a biological oxygen sensor: A new mechanism for heme-driven signal transduction, *Proc. Natl. Acad. Sci. U.S.A. 95*, 15177−15182.
27. Miyatake, H., Mukai, M., Park, S. Y., Adachi, S., Tamura, K., Nakamura, H., Nakamura, K., Tsuchiya, T., Iizuka, T., and Shiro, Y. (2000) Sensory mechanism of oxygen sensor FixL from *Rhizobium meliloti*: Crystallographic, mutagenesis and resonance Raman spectroscopic studies, *J. Mol. Biol. 301*, 415−431.
28. Gong, W., Hao, B., and Chan, M. K. (2000) New mechanistic insights from structural studies of the oxygen-sensing domain of *Bradyrhizobium japonicum* FixL, *Biochemistry 39*, 3955−3962.
29. Hao, B., Isaza, C., Arndt, J., Soltis, M., and Chan, M. K. (2002) Structure-based mechanism of O_2 sensing and ligand discrimination by the FixL heme domain of *Bradyrhizobium japonicum*, *Biochemistry 41*, 12952−12958.
30. Mukai, M., Nakamura, K., Nakamura, H., Iizuka, T., and Shiro, Y. (2000) Role of Ile209 and Ile210 on the heme pocket structure and regulation of histidine kinase activity of oxygen sensor FixL from *Rhizobium meliloti*, *Biochemistry 39*, 13810−13816.
31. Nakamura, H., Kumita, H., Imai, K., Iizuka, T., and Shiro, Y. (2004) ADP reduces the oxygen-binding affinity of a sensory histidine kinase, FixL: The possibility of an enhanced reciprocating kinase reaction, *Proc. Natl. Acad. Sci. U.S.A. 101*, 2742−2746.
32. Saito, K., Ito, E., Hosono, K., Nakamura, K., Imai, K., Iizuka, T., Shiro, Y., and Nakamura, H. (2003) The uncoupling of oxygen sensing, phosphorylation signaling and transcriptional activation in oxygen sensor FixL and FixJ mutants, *Mol. Microbiol. 48*, 373−383.
33. Gilles-Gonzalez, M. A., Gonzalez, G., Perutz, M. F., Kiger, L., Marden, M. C., and Poyart, C. (1994) Heme-based sensors,

exemplified by the kinaes FixL, are a new class of heme protein with distinctive ligand binding and autoxidation, *Biochemistry 33*, 8067−8073.
34. Nakamura, H., Saito, K., Ito, E., Tamura, K., Tsuchiya, T., Nishigaki, K., Shiro, Y., and Iizuka, T. (1998) Identification of the hydrophobic amino acid residues required for heme assembly in the rhizobial oxygen sensor protein FixL, *Biochem. Biophys. Res. Commun. 247*, 427−431.
35. Dou, Y., Admiraal, S. J., Ikeda-Saito, M., Krzywda, S., Wilkinson, A. J., Li, T., Olson, J. S., Prince, R. C., Pickering, I. J., and George, G. N. (1995) Alteration of axial coordination by protein engineering in myoglobin: Bisimidazole ligation in the His64 → Val/Val68 → His double mutant, *J. Biol. Chem. 270*, 15993−16001.
36. Fujii, H. (2002) ^{13}C NMR signal detection of iron-bound cyanide irons in ferric cyanide complexes of heme proteins, *J. Am. Chem. Soc. 124*, 5936−5937.
37. Goff, H. M., (1977) Carbon-13 nuclear magnetic resonance spectroscopy of iron(III) porphyrin−cyanide complexes. Location of the bound cyanide ion resonance, *J. Am. Chem. Soc. 99*, 7723−7725.
38. Morishima, I., and Inubushi, T., (1978) Nitrogen-15 nuclear magnetic resonance studies of iron-bound cyanide(nitrogen-15)-(1−) ion in ferric low-spin cyanide complexes of various porphyrin derivatives and various hemoproteins, *J. Am. Chem. Soc. 100*, 3568−3574.
39. Shiro, Y., Iizuka, T., Makino, R., Ishimura, Y., and Morishima, I., (1989) Nitrogen-15 NMR study on cyanide (C^{15}N-) complex of cytochrome P-450cam. Effects of d-camphor and putidaredoxin on the iron−ligand structure, *J. Am. Chem. Soc. 111*, 7707−7711.
40. Behere, D. V., Gonzalez-Vergara, E., and Goff, H. M., (1985) Unique cyanide nitrogen-15 nuclear magnetic resonance chemical shift values for cyano-peroxidase complexes. Relevance to the heme active-site structure and mechanism of peroxide activation, *Biochim. Biophys. Acta 832*, 319−325.
41. Behere, D. V., Ales, D. C., and Goff, H. M., (1986) Proton and nitrogen-15 NMR studies of ferricytochrome *c* cyanide complexes: Remarkable conservation of the heme environment among organisms of diverse origin, *Biochim. Biophys. Acta 871*, 285−292.
42. Nakamura, M., Ikeue, T, Fujii, H., and Yoshoumura, T., (1997) Change in electron configuration of ferric ion in bis(cyanide)-(*meso*-tetraalkylporphyrinatoiron(III)), [Fe(T*R*P)(CN)$_2$]$^-$, caused by the nonplanarity of the porphyrin ring, *J. Am. Chem. Soc. 119*, 6284−6291.
43. Balland, V., Bouzhir-Sima, L., Kiger, L., Marden, M. C., Vos, M. H., Liebl, U., and Mattioli, T. A. (2005) Role of arginine 220 in the oxygen sensor FixL from *Bradyrhizobium japonicum*, *J. Biol. Chem. 280*, 15279−15288.
44. Hirota S., Li, T., Phillips, G. N., Jr., Olson, J. S., Mukai M., and Kitagawa, T. (1996) Perturbation of the Fe−O$_2$ bond by nearby residues in heme pocket: Observation of ν_{Fe-O_2} Raman bands for oxymyoglobin mutants, *J. Am. Chem. Soc. 118*, 7845−7846.
45. Oldfield, T. J., Smerdon, S. J., Dauter, Z., Petratos, K., Wilson, K. S., and Wilkinson, A. J. (1992) High-resolution X-ray structures of pig metmyoglobin and two CD3 mutants: Mb(Lys45 → Arg) and Mb(Lys45 → Ser), *Biochemistry 31*, 8732−8739.
46. Brantley, R. E., Jr., Smerdon, S. J., Wilkinson, A. J., Singleton, E. W., and Olson. J. S. (1993) The mechanism of autoxidation of myoglobin, *J. Biol. Chem. 268*, 6995−7010.
47. Bertolucci, C., Ming, L. J., Gonzalez, G., and Gilles-Gonzalez, M. A. (1996) Assignment of the hyperfine-shifted ^{1}H NMR signals of the heme in the oxygen sensor FixL from *Rhizobium meliloti*, *Chem. Biol. 3*, 561−566.

BI051989A